Model Predictive Current Control of Single-Phase 13-Level Transistor-Clamped H-Bridge Based Cascaded Multilevel Inverter

K. Rameshkumar, V. Indragandhi, Geetha Mani and Padmanaban Sanjeevikumar

Abstract The manuscript presents a Model Predictive type Current Control (MPCC) of single-phase 13-level Transistor-Clamped H-Bridge (TCHB) based cascaded Multi Level Inverter (MLI) for improving power quality. The objective of the MPCC is to regulate the inverter output current by using 15 switches and 14 voltage vectors. The working condition of the MPCC strategy is investigated using steady state condition, transient state condition, variation of input frequency and variation of sampling time through simulations with RL load. The results show that the MPCC schemes perform well for all operating conditions and the inverter delivers a good quality of load voltage and load current with less harmonic components value. The inverter model and MPCC algorithm is implemented by using MATLAB software.

Keywords Cost function · Multi-level inverter · Predictive current control Sampling time · Total harmonic distortion

K. Rameshkumar (✉) · V. Indragandhi · G. Mani
School of Electrical Engineering, Vellore Institute of Technology (VIT) University, Vellore, Tamil Nadu, India
e-mail: rameshvel.k@gmail.com

V. Indragandhi
e-mail: indragandhi.v@vit.ac.in

G. Mani
e-mail: geethamani@gmail.com

P. Sanjeevikumar
Department of Electrical and Electronics Engineering, University of Johannesburg, Auckland Park, Johannesburg, South Africa
e-mail: sanjeevi_12@yahoo.co.in

A. Garg et al. (eds.), *Advances in Power Systems and Energy Management*, Lecture Notes in Electrical Engineering 436,
https://doi.org/10.1007/978-981-10-4394-9_58

1 Introduction

Multilevel Inverter (MLI) has become more significant interest among the researchers in recent years due to its significant performance. Different MLI topologies which are used such as MLI with neutral-point-clamped, MLI with diode clamped, cascaded H-bridge and flying capacitor MLI. On comparing with all other types of MLI, the cascaded H-bridge MLI has an advantages like its high reliability, modular structure, extendibility, enhanced fault capability and easy to alter the number of levels with minimum changes [1]. Nowadays, the TCHB based cascaded MLI inverter topology has more attention amongst researchers due to its simple methodology to increase levels of output by delivering different voltage levels by utilizing the capacitors arranged in a sequence manner. The traditional methods for control of MLI inverter uses multicarrier PWM control technique [2], hysteresis current control [3], Space Vector Modulation (SVM) [4], feed-forward SVM [5] and in [6] new modulation scheme is used to produce the gating signals.

Amongst the various control approaches utilized in power electronics, Model Predictive Control (MPC) strategy has increased level of popularity due to many advantages like good dynamic performance, improved current quality and the MPCC of converters has been extensively studied in the last decade and found some application in power converters like three phase two-level inverter [7], two-level inverter with four-leg inverter operating under balanced, unbalanced and nonlinear loading conditions were analyzed [8, 9] and this control techniques are also implemented on single-phase nine-level inverter [10], grid connected flying capacitor inverter [11], Three phase nested Neutral Point-Clamped (NPC) converter [12], three phase four-leg NPC converters [13–15], multilevel diode clamped inverter [16], multilevel cascaded H-bridge inverters [17], and grid connected cascaded H-bridge inverters [18], asymmetric flying capacitor converter [19] and direct matrix converter [20].

From the above references, by considering MPCC technique for single phase, three phase inverter and three phases MLI under several conditions is discussed. The analysis of single phase 13-level TCHB cascaded based MLI with MPCC for several conditions is not being described yet. So in this manuscript the MPCC technique has been applied to the single phase 13-level TCHB cascaded based MLI to analyze the steady state, transient state conditions, supply frequency variation and sampling time varying conditions. This manuscript is systematized as follows. In Sect. 2, the inverter model is presented. In Sect. 3, description of the MPCC strategy with algorithm is presented. In Sect. 4, simulation outcomes are discussed. Finally Sect. 5 concludes the work.

2 Inverter Modelling

A representation of a single phase model 13-level TCHB depends on cascaded MLI connected to the RL load is shown in Fig. 1. Three independent DC energy sources are consider in this study and three H-bridge sections and equal number of bidirectional switches to the bridge sections are used to generate a required voltage level on its output terminals. This MLI operation includes switching states with count of 14, which is alters from S_1 to S_{14}.

Then the voltage vector V_i can be derived from the MLI supply voltage V_{dc} and switching state S_i by

$$V_i = V_{dc}(S_{i4} - S_{i2}) * \left\{\frac{1}{2}S_{i5} + |S_{i1} - S_{i2}| \cdot |S_{i3} - S_{i4}|\right\} \tag{1}$$

where V_i, S_i are MLI voltage vectors and switching states of inverter respectively with $i = 1, 2 \ldots 14$.

The vector representation of inverter load current can be represented by

$$v = Ri + L\, \mathrm{d}i/\mathrm{d}t \tag{2}$$

In the above equation the L, R and v are the load inductance, load resistance and voltage vector by the MLI.

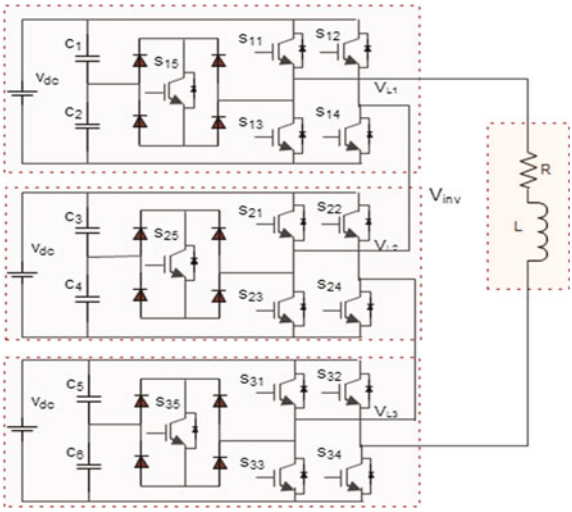

Fig. 1 Single-phase 13-level TCHB based cascaded MLI

3 Model Predictive Current Strategy

The MPCC scheme of MLI is presented in Fig. 2. Discrete system model, switching states and load current of MLI are taken to find out the upcoming variable performances to be regulated.

The system derivative $\frac{di}{dt}$ from Euler equation can be represented by

$$\frac{di}{dt} = \frac{i(k) - i(k-1)}{T_S} \tag{3}$$

Equation (3) is substituted in Eq. (2) the voltage vector can be represented by

$$v = Ri + L\frac{i(k) - i(k-1)}{T_S} \tag{4}$$

The inverter measured output current at the time of k is expressed by

$$i(k) = \frac{1}{RT_S + L} + [Li(k-1) + T_S v(k)] \tag{5}$$

Then the load current $i(k)$ is shifted in single step advance $i(k+1)$ and the predicted output current can be expressed by

$$i_p(k+1) = \frac{1}{RT_S + L} + [Li(k) + T_S v(k+1)] \tag{6}$$

In which $v(k+1)$ load voltage vector, and $i(k)$ is the monitored load current at the instant of k.

The most significant purpose of MPCC is to reduce the error among the references and a forecasted output load current which is defined as cost function or quality function (g). So in order to attain that objective, the inverter switching state

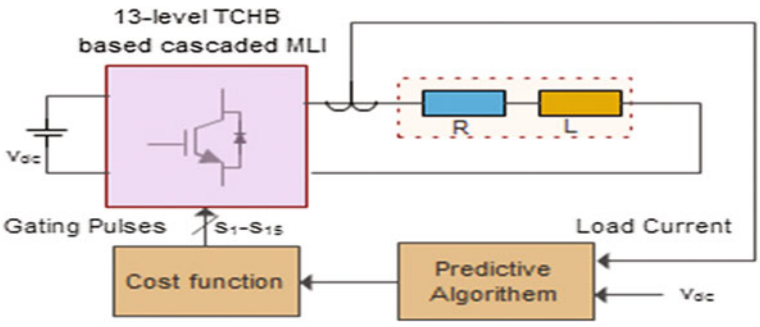

Fig. 2 Block diagram of MPCC of MLI

which is going to reduce 'g' is chosen and given at the time of next sampling instant.

In the subsequent sampling instant the difference among the reference load current and the predicted current of the load can be represented by

$$g = (i_{\text{Ref}}(k+1) - i_p(k+1)) \tag{7}$$

For computational simplicity absolute error is used in this manuscript. Other methods can be used to identify the cost functions such as error squared and it's represented as follows

$$g = (i_{\text{Ref}}(k+1) - i_p(k+1))^2 \tag{8}$$

Finally lowest of 'g' is selected and corresponding switching pulses is given as a gate pulse of the inverter. The detailed algorithm for control of MLI is as follows.

3.1 MPCC Algorithm for Inverter

The MPCC algorithm is implemented in MATLAB embedded function block. The functional block operates in the discrete update technique based on sampling time defined for the algorithm. The parameters used in this algorithm are shown in parameter initialization step, and each parameters are initialized with specific values (step 1). In step 2 the voltage vectors are estimated by using input supply voltage and 14 possible switching state and also the load current of inverter at specific value of (k + 1) are predicted by substituting eight voltage vectors and measured load current. The cost functions are calculated by relating the predicted current of load with the current reference as indicated in step 3. In step 4 cost function optimization is implemented. At last the switching state gives lowest 'g' which is selected and given to the MLI, as shown in step 5.

1. **Parameter initialization**
   Load Resistance = 150 Ω,
   Load inductance = 160 mH.
   Sampling frequency = 10 kHz
   Cost function at initial (g) = inf.
   Voltage vector at initial = V_1, and Switching state = S_1
2. **Voltage vector and load current prediction**
   $V_i = V_{\text{dc}}(S_{i4} - S_{i2}) * \left\{\frac{1}{2}S_5 + |S_{i1} - S_{i2}| \cdot |S_{i3} - S_{i4}|\right\} * /$ by using supply voltage and switching state $(S_1 - S_{14}) * /$
   Prediction of current at next instant
   $i_p(k+1) = \frac{1}{RT_S + L} + [L.i(k) + T_S v(k+1) /*$ considering inverter load current and voltage vector $(v_1 - v_{14})$*/

3. **Calculate '*g*' value**
   $g_{\text{value}} = (i_{\text{Ref}}(k+1) - i_p(k+1))$/* by using reference current and load current */
4. **Cost function optimization**

   If ($g < g_{\text{opt}}$) /*Optimum '*g*' and choice of choosing the switching state*/
   Updating optimal cost function and switching state

$$g_{\text{opt}} = g;$$
$$x_{\text{opt}} = i;$$

5. **Optimum switching state**
   $S_a = S(x_{\text{opt}}, 1)$; /*optimal switching state is given to inverter*/
   $S_b = S(x_{\text{opt}}, 2)$;
   $S_c = S(x_{\text{opt}}, 3)$;
   The optimal switching pulse obtained is given to the inverter.

4 Simulation Results

The operation of MPCC based Single-Phase 13-level TCHB based MLI under four different analysis has been taken and simulated in MATLAB/Simulink software. The parameters for inverter and load are indicated in Table 1. The reference current is defined manually. The concepts of MPCC and inverter model are discussed previously.

4.1 Steady State Analysis

In this analysis the MPCC technique is applied to the MLI with constant load and reference condition. Here the reference current amplitude is fixed as 2 A and inverter DC-Link voltage to be maintained at 120 V for each level. Figure 3

Table 1 Inverter and load parameters

Parameters	Value
Input voltage V	360 V (120 V for each level)
Frequency	50 Hz
Sampling time (T_s)	100 μs
Load resistance	160 Ω
Load inductance	160 mH
DC-link capacitor value	3300 μF

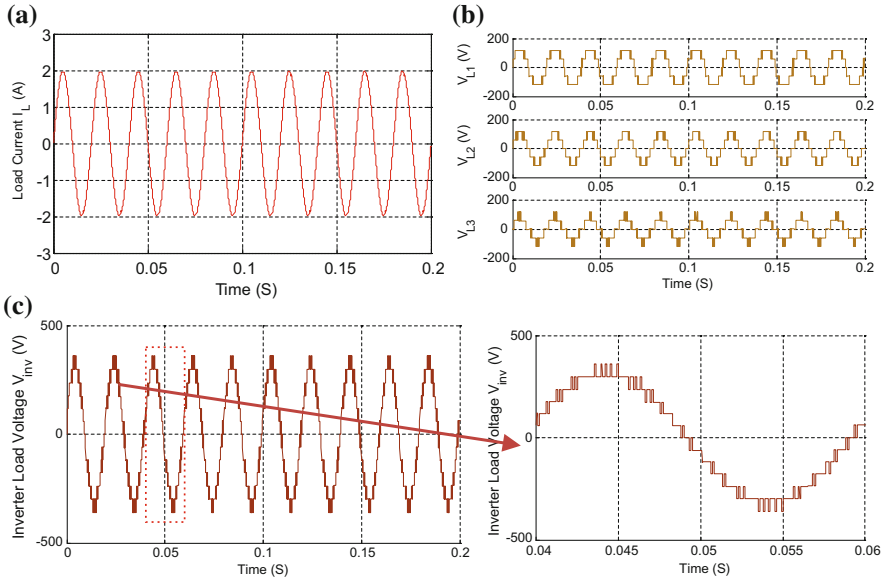

Fig. 3 Illustrates the simulation results concerning steady state response. **a** Load current, **b** inverter voltage at each level and **c** inverter load voltage

illustrates the simulated outcome of the load current, resultant output voltage 'V_{inv}' and voltage at each level (V_{L1}, V_{L2}, V_{L3}).

4.2 Transient State Response

In transient state condition, two different conditions are evaluated. In the first condition the reference current amplitude increases from 0 to 2 A at 0.04 s and consecutively current reference decreases from 2 to 1.5 A at 0.12 s with R = 160 Ω, L = 160 mH which is shown in Fig. 4.

In the second condition the current reference amplitude is fixed by 2 A with frequency of 50 Hz and the load resistance value changes from 150 to 165 Ω at 0.04 s and consecutively loads resistance changes from 165 to 175 Ω at 0.12 s that is depicted in Fig. 5. The result shows that the measured output current tracks its reference current instantly without any under or overshoot.

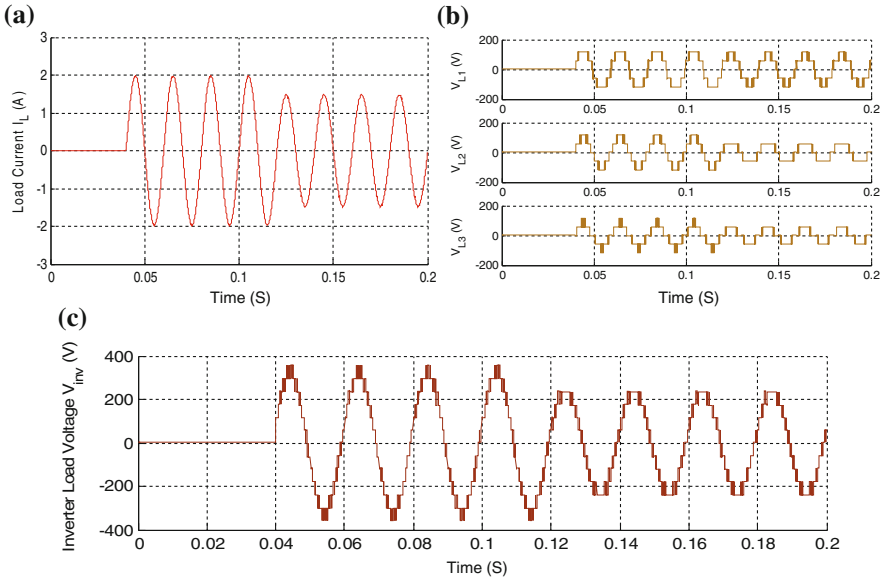

Fig. 4 Illustrates the simulation results concerning transient response of **a** load current, **b** inverter voltage at each level and **c** inverter load voltage

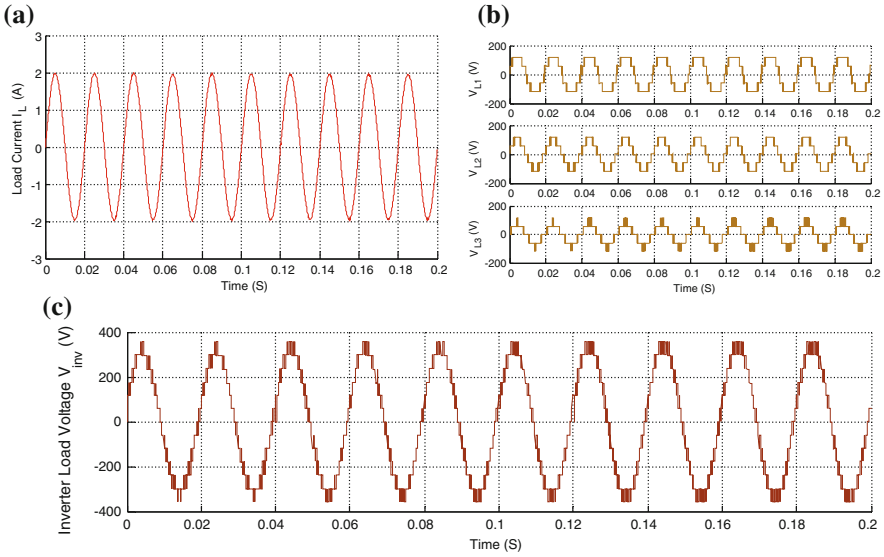

Fig. 5 Illustrates the simulation results concerning transient response of **a** load current, **b** inverter load voltage at each level and **c** inverter load voltage

4.3 Examination with Supply Frequency Variations

In this examination the reference current frequency changes from 50–100 Hz at 0.04 s and consecutively reference current frequency changes from 100 to 20 Hz at 0.11 s with R = 160 Ω, L = 160 mH. Figure 6 clearly shows that the load current tracks the reference with no overshoot.

4.4 Examination with Sampling Time Variations

The examination is tested by varying the sampling time, in that the output current and voltage THD varies according to the sampling time variation. The FFT analysis for inverter output current and voltage is given in Figs. 7 and 8. When the sampling time was set as 50 µs the THD shows 0.42% for current; 9.92% for voltage. However while increasing the sampling period from 100, 150 and 200 the THD for load current and load voltage also increases gradually as shown in Table 2.

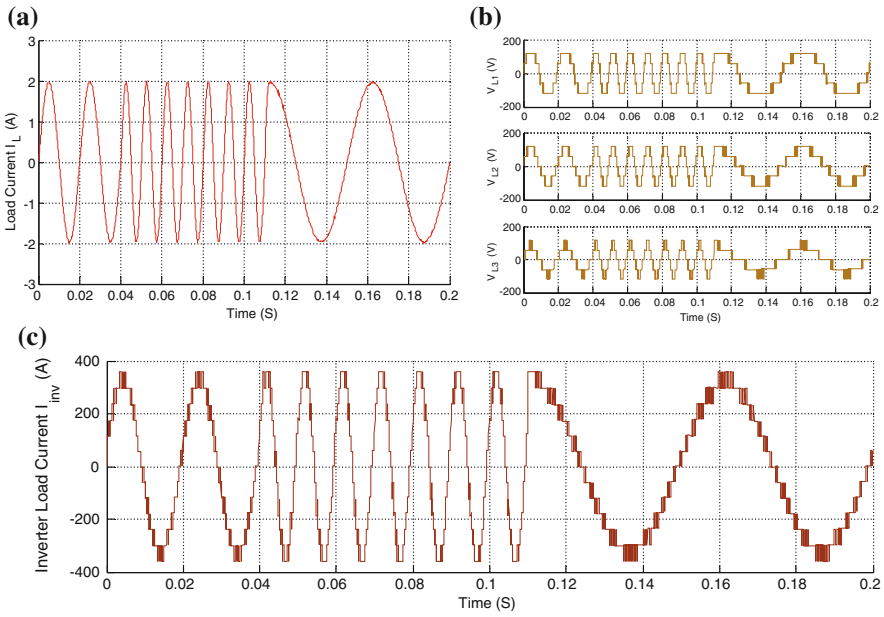

Fig. 6 Illustrates the simulation results concerning transient response of **a** load current, **b** inverter load voltage at each level and **c** inverter load voltage

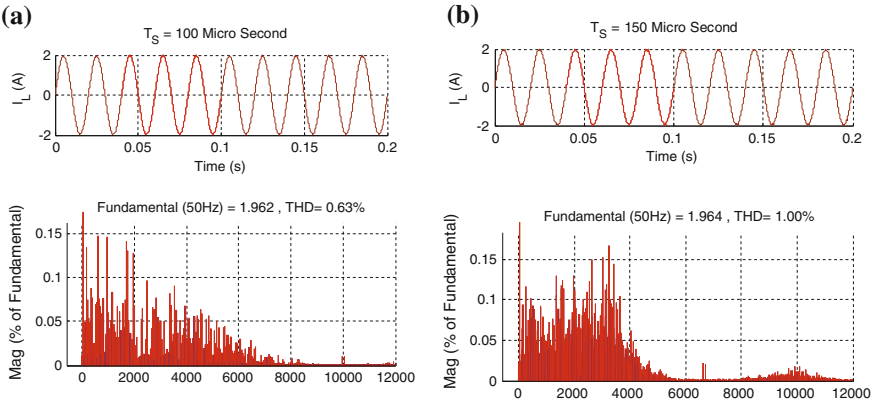

Fig. 7 THD for the load current with the sampling time of **a** 100 µs and **b** 150 µs

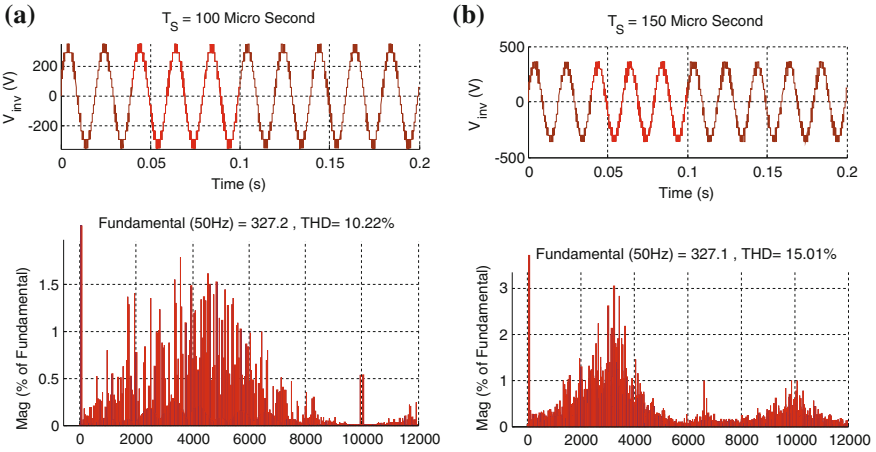

Fig. 8 THD for the load voltage with the sampling time of **a** 100 µs and **b** 150 µs

Table 2 THD for load current and load voltage with different sampling time

Sampling time T_s (µs)	THD %	
	Load current	Load voltage
50	0.42	9.92
100	0.63	10.22
150	1.0	15.01
200	2.2	32.74

5 Conclusion

The MPCC of single-phase 13-level TCHB based cascaded MLI was designed and analyzed with MATLAB Simulink model. And also, the performance indices i.e., steady state, transient state conditions, variation of reference current frequency and sampling time are exhibited with corresponding simulation results. It is proved that this control technique is simple and easy to exhibit in real time and straightforwardly prolonged to other type of converters with various applications, though it does not have a complex design and any modulating stages.

References

1. Halim, W.A., Rahim, N.A., Azri, M.: Selective harmonic elimination for a single-phase 13-level TCHB based cascaded multilevel inverter using FPGA. J. Power Electr. **14**, 488–498 (2014)
2. McGrath, B.P., Holmes, D.G.: Multicarrier PWM strategies for multilevel inverters. IEEE Trans. Industr. Electr. **49**, 858–867 (2002)
3. Shukla, A., Ghosh, A., Joshi, A.: Hysteresis current control operation of flying capacitor multilevel inverter and its application in shunt compensation of distribution systems. IEEE Trans. Power Deliv. **22**, 396–405 (2007)
4. Celanovic, N., Boroyevich, D.: A fast space-vector modulation algorithm for multilevel three-phase converters. IEEE Trans. Ind. Appl. **37**, 637–641 (2001)
5. Leon, J.I., Vazquez, S., Watson, A.J., Franquelo, L.G., Carrasco, J.M.: Feed-forward space vector modulation for single-phase multilevel cascaded converters with any DC voltage ratio. IEEE Trans. Industr. Electr. **56**, 315–325 (2009)
6. Rodríguez, J., Pontt, J., Correa, P., Silva, C.: A new modulation method to reduce common-mode voltages in multilevel inverters. IEEE Trans. Industr. Electr. **51**, 834–839 (2004)
7. Rodríguez, J., Pontt, J., Silva, C.A., Correa, P., Lezana, P., Cortes, P., Ammann, U.: Predictive current control of a voltage source inverter. IEEE Trans. Ind. Electr. **54**, 495–503 (2007)
8. Yaramasu, V., Rivera, M., Wu, B., Rodríguez, J.: Model predictive current control of two-level four-leg inverters—Part I: Concept, algorithm and simulation analysis. IEEE Trans. Power Electr. **28**, 3459–3468 (2013)
9. Rivera, M., Yaramasu, V., Rodríguez, J., Wu, B.: Model predictive current control of two-level four-leg inverters—Part II: Experimental implementation and validation. IEEE Trans. Power Electr. **28**, 3469–3478 (2013)
10. Kakosimos, P., Pavlou, K., Kladas, A., Manias, S.: A single-phase nine-level inverter for renewable energy systems employing model predictive control. Energy Convers. Manag. **89**, 427–437 (2015)
11. Trabelsi, M., Ghazi, K.A., Emadi, N.A., Brahim, L.B.: A weighted real-time predictive controller for a grid connected flying capacitors inverter. Electr. Power Energy Syst. **49**, 322–332 (2013)
12. Narimani, M., Wu, B., Yaramasu, V., Cheng, Z., Zargari, N.R.: Finite control-set model predictive control (FCS-MPC) of nested neutral point-clamped (NNPC) converter. IEEE Trans. Power Electr. **30**, 7262–7269 (2015)

13. Yaramasu, V., Rivera, M., Narimani, M., Wu, B., Rodríguez, J.: Finite state model-based predictive current control with two-step horizon for four-leg NPC converters. J. Power Electr. **14**, 1178–1188 (2014)
14. Vargas, R., Cortes, P., Ammann, U., Rodríguez, J., Pontt, J.: Predictive control of a three-phase neutral-point-clamped inverter. IEEE Trans. Ind. Electr. **54**, 2697–2705 (2007)
15. Yaramasua, V., Riverab, M., Narimania, M., Wu, B., Rodríguez, J.: High performance operation for a four-leg NPC inverter with two-sample-ahead predictive control strategy. Electr. Power Syst. Res. **123**, 31–39 (2015)
16. Yaramasu, V., Wu, B., Rivera, M., Narimani, M., Kouro, S., Rodríguez, J.: Generalized approach for predictive control with common-mode voltage mitigation in multilevel diode-clamped converters. IET Power Electr. **8**, 1440–1450 (2015)
17. Cortes, P., Wilson, A., Kouro, S., Rodríguez, J., Abu-Rub, H.: Model predictive control of multilevel cascaded H-bridge inverters. IEEE Trans. Ind. Electr. **57**, 2691–2699 (2010)
18. Han, J., Li, C., Yang, T., Han, J.: Simplified finite set model predictive control strategy of grid-connected cascade H-bridge converter. J. Control Sci. Eng. (2016)
19. Lezana, P., Aguilera, R., Quevedo, D.: Model predictive control of an asymmetric flying capacitor converter. IEEE Trans. Ind. Electr. **56**, 1839–1846 (2009)
20. Rivera, M., Rojas, C., Rodridguez, J., Wheeler, P., Wu, B., Espinoza, J.: Predictive current control with input filter resonance mitigation for a direct matrix converter. IEEE Trans. Power Electr. **26**, 2794–2803 (2011)